Significance of Orthotropic Material Models to Predict Stress Around Bone-Implant Interface Using Numerical Simulation

Pankaj Dhatrak[1,2] · Vedant Girme[1,2] · Uddhav Shirsat[3] · S. Sumanth[4] · Vijay Deshmukh[5]

Abstract

Several finite element models of bone-implant prosthetic derived with geometrical topology and material properties. Most of them adopted linear isotropic material properties to predict stresses around bone-implant interface. The objective of the present study is to compare stress distribution around bone-implant interface between two material models. In order to understand the biomechanical stress behavior at bone-implant interface, four different implant models were selected for the study. Mandibular bone section material models for isotropic and orthotropic material is defined with the contact between bone and implant surface to predict the von Mises stresses in the cancellous and cortical bone under the influence of vertical load of 100 N (coronal-apical), lateral load of 40 N (mesial-distal), and oblique load of 100 N at 45° to the axis of implant on crown surface. A nonlinear Abaqus CAE code is used to predict stresses distribution comparison between two material models.

The current study compares the result of stress in cancellous and cortical bone with isotropic and orthotropic material models. The stress distribution along the interface was presented for vertical, lateral, and oblique loading of selected implant models. Finite element (FE) numerical simulation result shows that the orthotropic material model is more acceptable than the isotropic material model to predict stress along bone-implant interface.

Keywords Bone-implant interface · Isotropic · Orthotropic · Stress analysis

1 Introduction

Dental implant system is extensively used in place of missing or damaged natural tooth in the field of dentistry. Finite element analysis (FEA) is one of the most common and useful numerical method that provides precise stress distribution field around bone-implant interface [1, 2]. It is primarily used to predict the mechanical behavior of dental implant and the factors that influence the behavior of implant [3, 4]. Whenever precise properties are insignificant, simpler models can be used for research [5]. Simplified isotropic material models cannot determine stress accurately. It provides general insight into the biomechanics of implants under applied load conditions [6]. Thus, FEA has been proved as a useful tool in various mechanobiological interdisciplinary studies.

Modern study in dentistry has improved the understanding of implants and specifically dental reconstruction [7, 8]. Branemark defined osseointegration as integration of titanium implant with bone tissues when placed in the jaw bone [9, 10]. The osseointegration is the structural and functional integration between bone and implant surface [11]. The integration provides a binding mechanism that incorporates a component of a foreign material when placed inside the human body [12].

The use of FEA in the field of biomechanics has changed since it was first introduced. Increasing efforts are being made to replicate the actual bone materials [13]. During mastication, the human jaw mandible is subjected to different forces [14]. Determination of stress-strain induced in bone is barely governed through in vivo study. However, validation using numerical

✉ Pankaj Dhatrak
pankaj.dhatrak@mitwpu.edu.in

1 Research Scholar ZCOER, MIT-WPU, Pune 411038, India

2 School of Mechanical Engineering Dr. Vishwanath Karad MIT-WPU (Formerly MAEER'S MIT, Pune), Pune 411038, India

3 Department of Mechanical Engineering, Dhole Patil College of Engineering, Pune 412207, India

4 Department of Periodontic, M. A. Rangoonwal College of Dental Science and Research Centre, Pune 411001, India

5 International Clinical Dental Research Organisation, Pune 411038, India

Fig. 1 3D FE mesh model of commercial implant system. Model A, Nobel implant; Model B, Ankylos implant; Model C, Biohorizon implant; Model D, Xive implant

Model A   Model B   Model C   Model D
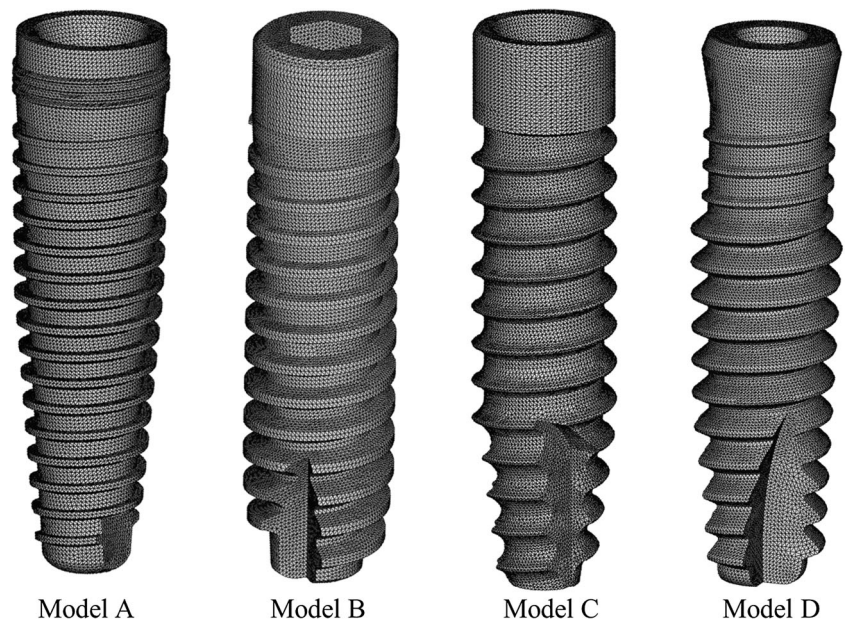
simulation depends on number of other factors [15]. FE model should be simulated to the real bone structure in consideration. Simplified FE geometry, simplified material properties, and inappropriate boundary conditions lead to unrealistic FEA results [16, 17].

Most of the earlier studies assume linear isotropic material properties for simplicity in FE model. But recently, the bone material is considered as more of an orthotropic material than an isotropic material and such orthotropic material property is now being considered in recent studies [18]. Therefore, it is necessary to know the significance of material models on stress distribution along bone-implant interface in numerical simulation [19]. In present study, stress analysis of four different titanium dental implants is compared considering isotropic material and orthotropic material properties.

2 Methodology

2.1 Model Generation

A computer tomography (CT) scan data provide appropriate topology of the bone under consideration depending on the bone and the surrounding tissues [19, 20]. Hounsfield unit is a quantitative scale which provides precise density of the bone. Replication of a bone structure highly depends on the quality of the CT scan. In several approaches, the correlation of bone stiffness and attenuation is used. Further, the DICOM-files comprising of the sectional slices attained from the CT scanner are imported into an editing software, namely, AMIRA. AMIRA's image segmentation editor consists of several tools for marking/labelling the bony structures in the CT-scans. Post
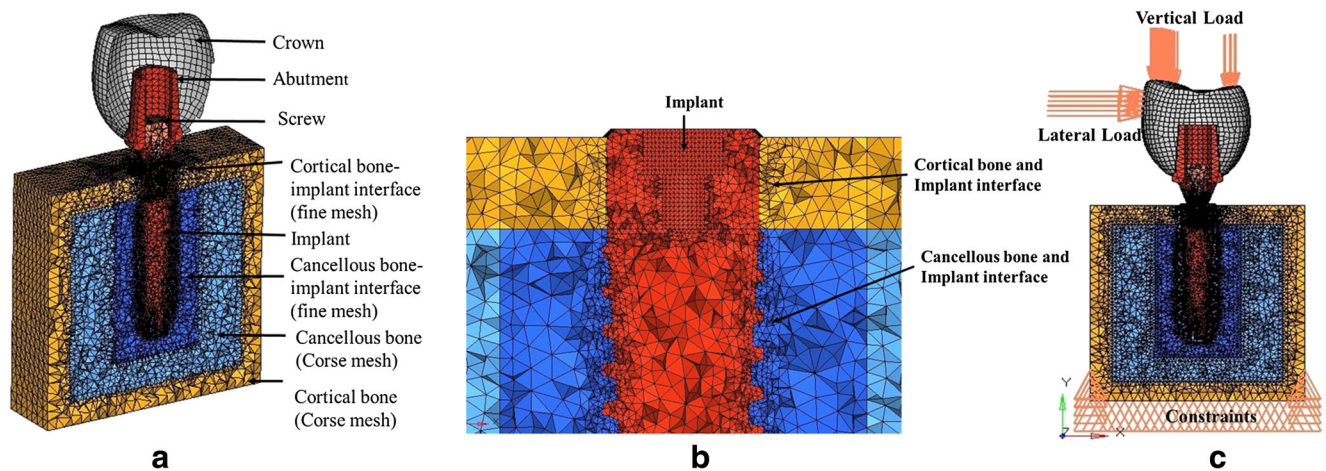

Fig. 2 Half cut-section of FE model. **a** FE mesh model of implant prosthetic with bone. **b** Enlarge view of mesh refinement at implant-bone interface. **c** Loading and boundary condition applied on the surface of crown

Table 1 Material properties used for isotropic model

Material constant	Implant, abutment, screw	Crown	Cortical bone	Cancellous bone
E (MPa)	110,000	70,000	22,800	1148
μ	0.35	0.19	0.3	0.3

labelling, a three- dimensional replica of bone structure with triangulated faces is automatically generated. [21]. There is a linear relationship between CT number and Hounsfield unit (HU) with reference to bone material properties. [22]. Moreover, Hounsfield scale has a linearity with apparent density of bone [23]. Using different modeling techniques, several FEA models have been introduced with topology and material properties derived from CT data [24–26].

The stereo-lithographic (STL) format of the geometric prototype of mandibular jawbone can be generally obtained from the CT scan. The geometrical model in STL format can be converted into a three-dimensional surface model using commercially available software. [16] Such software allows automatic generation of outer surface of jaw bone. Based on previous literature, a simplified jaw bone model positioned below the right lower first molar having dimensions $10 \times 20 \times 30$ mm was build. This segment after converting into a geometrical model was separated according to the cortical and cancellous bone properties. Thickness of the cortical bone was considered to be 2 mm and is assumed to be constant throughout. Furthermore, a 3D CAD model of four commercially used dental implants (as shown in Fig. 1) having dimensions of 3.5 mm diameter and 15.0 mm length is then inserted into generated segment of the jaw bone. The cut section of finite element model of the implant prosthetics is shown in Fig. 2a.

2.2 Mesh Generation

In this study, all four implant model are meshed using tetrahedral elements. FE mesh model generation using hexahedral elements gives maximum accuracy in minimal computational time especially in contact problems. Some of its disadvantages are the impediments of generating these elements which are very intricate and time-consuming [21]. Most of the literature states that linear

hexahedral element gives similar accuracy to that of quadratic tetrahedral elements. Consequently, implant prosthetic (implant, abutment, screw) with cancellous and cortical bone are meshed with a quadratic tetrahedral solid element (C3D10) [27]; however, the crown is modeled using shell element (S3R and S4R). The average element size of 0.05 mm is defined to provide an adequate accuracy by mesh convergence test [28]. The bone-implant interface with fine mesh is used to improve the accuracy in FE simulation as shown in Fig. 2b. The generated assembly is then transferred to Abaqus CAE code (ABAQUS V6.10-1) [29]. Abaqus CAE code is a numerical computer-aided engineering simulation software–based finite element method (FEM) which provides solution to linear and nonlinear problems.

3 Isotropic and Orthotropic Models

3.1 Modeling of Bone

Two most commonly used materials for modeling of cortical and cancellous bone are isotropic and orthotropic. Due to extensive inhomogeneity, an isotropic modeling is really an inappropriate approximation to the real behavior of the bone. Thus, it should be modeled as an orthotropic material which will give a more realistic behavior.

$$\begin{bmatrix} D_{1111} & D_{1122} & D_{1133} & 0 & 0 & 0 \\ D_{2211} & D_{2222} & D_{2233} & 0 & 0 & 0 \\ D_{3311} & D_{3322} & D_{3333} & 0 & 0 & 0 \\ 0 & 0 & 0 & D_{1212} & 0 & 0 \\ 0 & 0 & 0 & 0 & D_{1313} & 0 \\ 0 & 0 & 0 & 0 & 0 & D_{2323} \end{bmatrix}$$

Fig. 3 D matrix consisting of elastic stiffness parameters

Table 2 Material properties used for orthotropic model

Material properties		Cancellous bone	Cortical bone
	E_1	210	12,700
Elastic moduli	E_2	1148	17,900
(MPa)	E_3	1148	22,800
	G_{12}	68	5000
Shear moduli	G_{13}	68	5500
(MPa)	G_{23}	434	7400
	μ_{12}	0.055	0.18
	μ_{21}	0.105	0.35
Poisson's ratio	μ_{13}	0.055	0.31
	μ_{31}	0.093	0.49
	μ_{23}	0.322	0.28
	μ_{32}	0.325	0.31

Table 3 Values of different material stiffness parameters

Material stiffness parameter (MPa)	Cancellous bone	Cortical bone
D_{1111}	213.49	18,487.3
D_{2222}	1296.83	24,158.2
D_{3333}	1295.97	34,096.5
D_{1122}	32.18	9920.63
D_{1133}	30.31	12,321.7
D_{2233}	426.39	10,560.1
D_{1212}	68	5000
D_{1313}	68	5500
D_{2323}	434	7400

3.1.1 Isotropic Model

Isotropic materials have identical material properties in all directions and can therefore be easily defined. Several literatures provide a range of isotropic material properties of a cancellous and cortical bone. Thus, values of elastic properties of implant prosthetic and jaw bone [16, 17] have been summarized in the Table 1.

3.1.2 Orthotropic Model

Two material models which had same boundary conditions but different material properties were used. Using FEA approach, the isotropic material model was established which consist of assigning material properties, prominent boundary conditions and then solving the FE model with numerical simulation. Some of the researchers accepted bone anisotropy is a complex orthotropy [17]. Orthotropic material model was established by assigning material properties in an arbitrary direction and then solving for three different loading conditions in order to define the final direction of axes of orthotropy. With these direction defined and applied to each element, a final solution was obtained [30]. Local orientation of the orthotropic material models along the bone anatomy is based on direction of principal stresses formed by masticatory forces and distinct boundary conditions. The properties are aligned with highest principal stresses in orthotropic material model. However, orthotropic material orientation rival closely the bone structure, experimental validation of mechanical behavior needs to be implemented.

Orthotropic materials have different material properties in mutually perpendicular directions. Linear elasticity in orthotropic materials can be defined by D matrix consisting of 9 independent elastic stiffness parameters [31], as shown in Fig. 3 where $D_{1122} = D_{2211}$, $D_{1133} = D_{3311}$, and $D_{2233} = D_{3322}$.

Elastic stiffness parameters for an orthotropic model were calculated using Eqs. 1–10. These equations are the functions of elastic moduli, shear moduli, and Poisson's ratio [16, 17] the values of which are summarized in Table 2. The calculated elastic stiffness parameters are summarized in Table 3.

$$D_{1111} = E_1\left(1 - \mu_{23} \times \mu_{32}\right) \Upsilon \tag{1}$$

$$D_{2222} = E_2\left(1 - \mu_{13} \times \mu_{31}\right) \Upsilon \tag{2}$$

$$D_{3333} = E_3\left(1 - \mu_{12} \times \mu_{21}\right) \Upsilon \tag{3}$$

$$D_{1122} = E_1\left(\mu_{21} - \mu_{31} \times \mu_{23}\right) \Upsilon \tag{4}$$

$$D_{1133} = E_1\left(\mu_{31} - \mu_{21} \times \mu_{32}\right) \Upsilon \tag{5}$$

$$D_{2233} = E_2\left(\mu_{32} - \mu_{12} \times \mu_{31}\right) \Upsilon \tag{6}$$
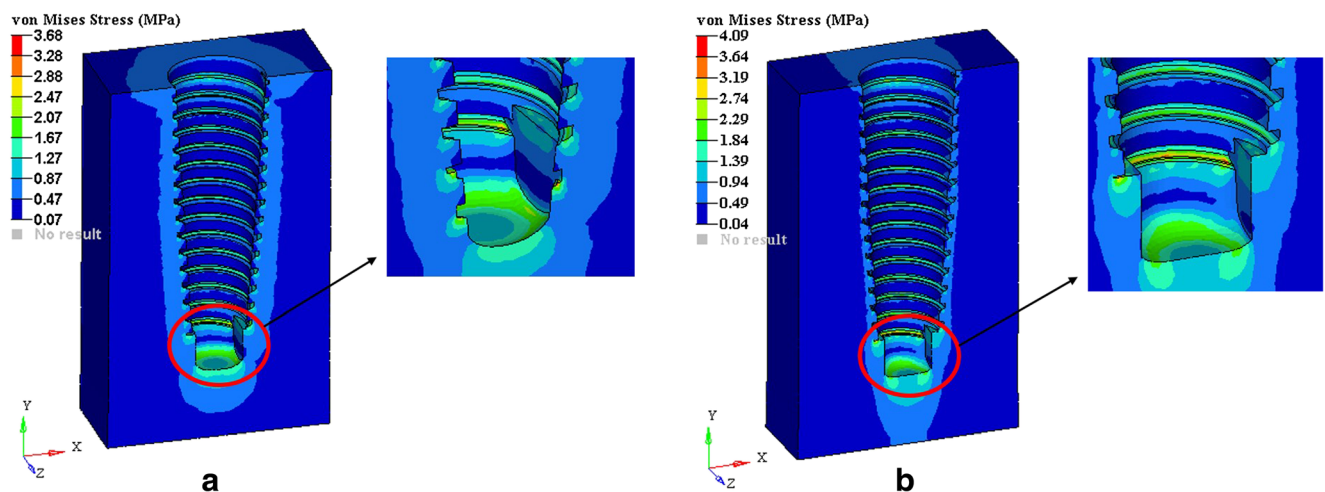
$$D_{1212} = G_{12} \tag{7}$$

Fig. 4 FEA von Mises plot of Model A (vertical load): **a** Isotropic material model. **b** Orthotropic material model
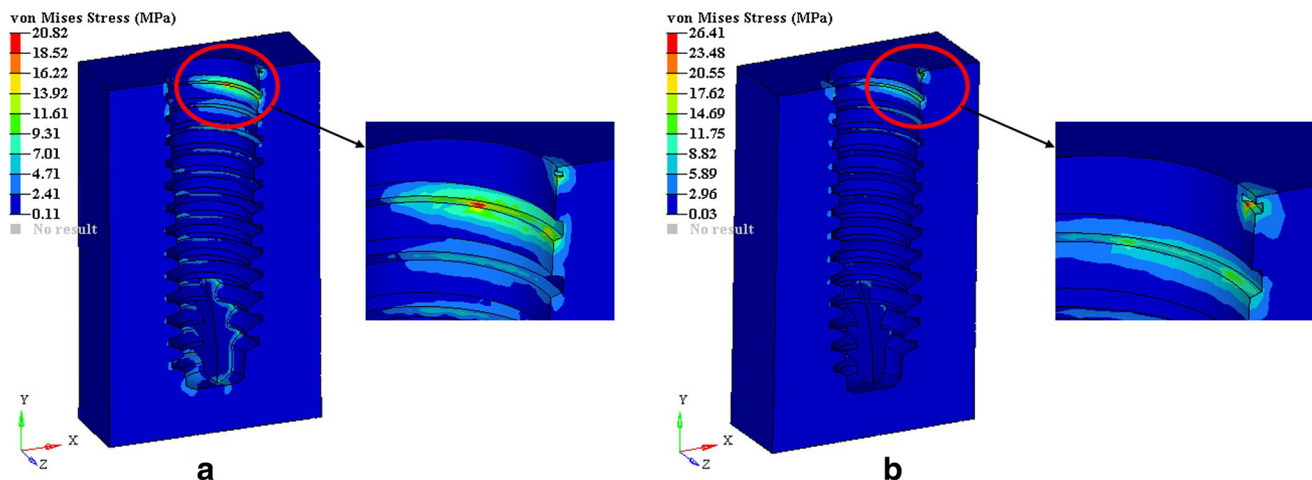
Fig. 5 FEA von Mises plot of Model B (oblique load): **a** Isotropic material model. **b** Orthotropic material model

$$D_{1313} = G_{13} \tag{8}$$

$$D_{2323} = G_{23} \tag{9}$$

$$\Upsilon = 1/(1-(\mu_{12} \times \mu_{21})-(\mu_{23} \times \mu_{32})-(\mu_{31} \times \mu_{13})-(2\mu_{21} \times \mu_{32} \times \mu_{13})) \tag{10}$$

4 Load and Boundary Conditions

Three loading condition were simulated in the present study to find the stress distribution along bone-implant interface. All four implant were modeled with a vertical load (coronal-apical) of 100 N, lateral load (mesial-distal) of 40 N and oblique load 100 N at 45° to the axis of implant on crown surface. [28, 32]. The bottom nodes of cortical bone are constrained with zero degree of freedom. The oblique load resolved into its vertical and lateral component is applied on crown surface as shown in the Fig. 2c.

5 FE Results

Figures 4, 5, 6, and 7 depict the von Mises stress results of cancellous and cortical bone for both isotropic and orthotropic

material models. The stress distribution pattern for all four models is found to be similar with respect to material models used. For Model A with isotropic material properties, the von Mises stress in cancellous bone is 11.14% lesser (which is least value in all four models) than the orthotropic material properties (Fig. 4a, b. For Model B with isotropic material properties, the von Mises stress in cancellous bone is 48.49% more (which is the maximum value in all four implant models) than the orthotropic material properties (Fig. 5a, b).

Similarly, for Model C with isotropic material properties, the von Mises stress in cortical bone is 15.94% lesser (which is the least value in all four model) than the orthotropic material properties (Fig. 6a, b). For Model D with isotropic material properties, the von Mises stress in cortical bone is 16% more(which is the maximum value in all four models) than the orthotropic material properties (Fig. 7a, b).

Bone adaption and bone growth variation shows prominent effect on stress and strain relationship. Biomechanical behavior of bone subjected to masticatory force notably differs between the types of bone modeling. The von Mises stress in bone density–dependent orthotropy model is higher in comparison with other model [16]. With few exceptions, orthotropic material model stress result shows maximum von Mises stress at a point of interest is consider instead of principle stress.

Fig. 6 FEA von Mises plot of Model C (vertical load): **a** Isotropic material model. **b** Orthotropic material model
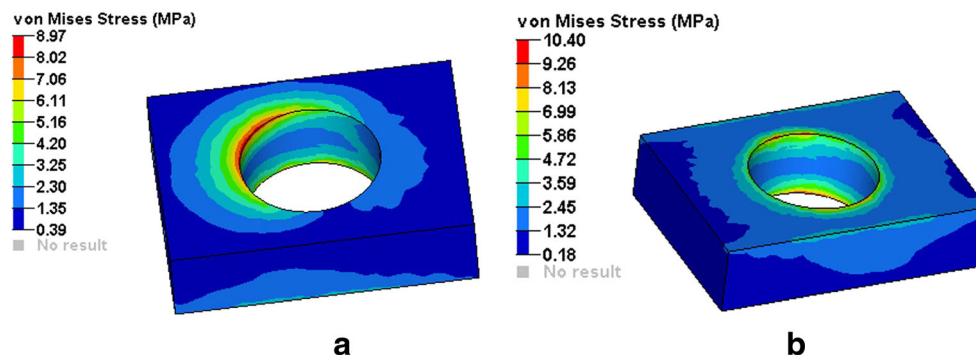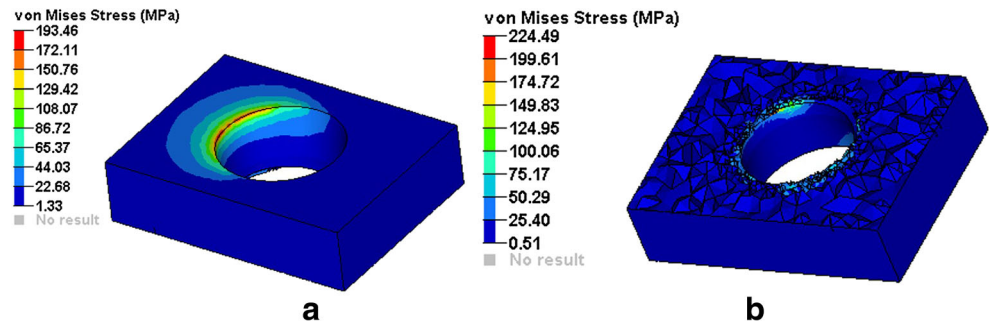
Fig. 7 FEA von Mises plot of Model D (oblique load): **a** Isotropic material model. **b** Orthotropic material model

Comparison between the isotropic and orthotropic material model results are presented in Figs. 8, 9, and 10. For vertical load, the orthotropic material properties show higher value of von Mises stress for all types of model used. Model A and Model C show close agreement for both material models whereas Model B and Model D show higher stresses in lateral loading condition. Model A, C, and D also show maximum value of stresses in orthotropic material model except Model B in oblique loading.

6 Discussion

A human bone is of great physiological importance to support the implant for better osseointegration, which depends on biomechanical behavior of bone. The mandibular bone behaves as anisotropic material. However, the different material model affects the stresses at bone-implant interface [21]. Numerical simulation results using both isotropic and orthotropic material models depend on similarity of each of these models to the real jaw bone material properties. It is well known that the jaw bone exhibits orthotropic material properties; still, most of the researchers adopted simplified isotropic material models. Human jaw bone behavior can be modeled as orthotropic or anisotropic material property depending on apparent density [16]. In the present work, comparative isotropic and orthotropic material models under three specific loading conditions are used to

predict stresses at the bone-implant interface. Previous literatures showed the stresses at bone-implant interface may vary depending on different material models. The orthotropic material model closely resembles the human bone properties and greatly improves biomechanical behavior which improve accuracy in numerical simulation. Recently, Xi Ding et al. investigated the influence of orthotropic material in completely dentate mandible and subsequently on resultant stresses. Based on orthotropic material properties of cancellous and cortical bone, FE model is generated. The von Mises stress in bone density–dependent orthotropy model is higher in comparison with other model [16]. The increase in von Mises Stresses is seen in orthotropic material models as compared to isotropic material models, similar to the result of Xi Ding et al. [17]. Bone adaption and bone growth variation shows prominent effect on stress and strain relationship. Biomechanical behavior of bone subjected to masticatory force notably differs between the types of bone modeling. Based on previous literature, the von Mises stress criteria is used to compare stress in cancellous and cortical bone with two material model of interest.

Recent works on drug delivery and gene manifestation demonstrated the need for cell growth formation/modification [33, 34]. Microchambers composed of polylactic acid (PLA) array thin film coating is used to encapsulate small hydrophilic cargo in less than 1 h [35, 36]. Biocompatible and biodegradable PLA thin film composite are mostly
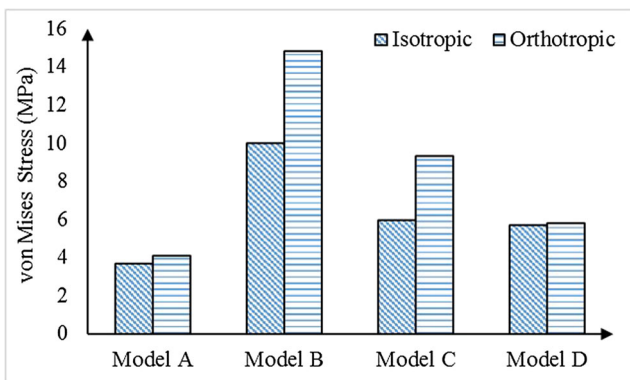

Fig. 8 FEA and experimental stress intensity comparison under 100 N occlusal load
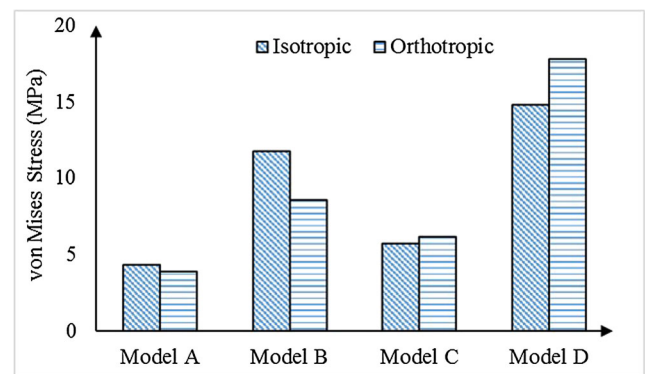

Fig. 9 FEA and experimental stress intensity comparison under 40 N Lateral load
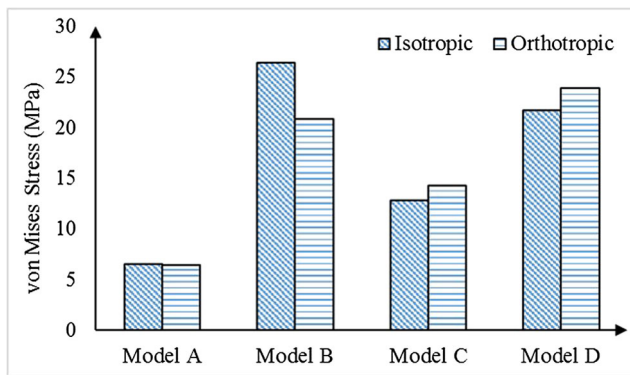
Fig. 10 FEA and experimental stress intensity comparison under oblique load of 100 N at 45°

appropriate coating materials to prevent implant related infection [37]. Titanium implant with different biomaterial base surface coating is used to improve healing time [37]. Hydroxyapatite (HA) biocomposite–coated implants were used in part with limited success, and have shown a phenomenon called bio-integration. Recently, many studies are trying drug-coated implants which accelerate the bone formation leading to further osseointegration, resulting in better acceptability by patients. The results from this study demonstrated implication of orthotropic material model without considering the implant coating effects on stress distribution. A future, more detailed study should consider the implant-coating effects on stress distribution due to variation in bone remodeling process.

FE numerical simulation shows the maximum von Mises stress at the top region of cancellous bone for applied lateral and oblique loading condition, independent of the type of material model used. The stress distribution pattern along the bone-implant interface in isotropic and orthotropic material models shows similar to that of Franci Gačnik et al. [16]. The maximum von Mises Stress in the cortical bone is also much higher when predicted by orthotropic material model as compared to isotropic material model. For vertical load, the average percentage (all four model) increase in von Mises Stresses of cancellous and cortical bone in orthotropic material property is 29.79% and 25.11% respectively. Similarly, for oblique loading, the average percentage increase in von Mises Stress of cancellous and cortical bone in orthotropic material model is up to 1.69% and 6.5% respectively. Thus, it was noticed that the orthotropic material model had a more profound effect on the cancellous bone in vertical loading, whereas it had a more profound effect on cortical bone in case of oblique loading. This indicates that the predicted von Mises stresses in isotropic material models are comparatively lower than orthotropic material model which is expected in reality. In FE numerical simulation, the orthotropic material model is more acceptable than the isotropic material model to predict stress along bone-implant interface.

7 Conclusions

FE numerical simulation result shows that the orthotropic material model is more acceptable than the isotropic material model to predict stress along bone-implant interface. In comparison with isotropic material models, orthotropic material model exhibits an accurate stress distribution in human mandibular bone. The used elastic parameter orthotropic material model of a human mandibular bone can be recommended for further research in dental implant stress analysis as it provides realistic approach in numerical simulation.

Compliance with Ethical Standards

Conflict of Interest   None

Research Involving Humans and Animals Statement   None.

Informed Consent   None.

Funding Statement   None.

Nomenclature D, elastic stiffness parameter; E, elastic modulus, N/mm²; G, shear moduli, N/mm²; μ, Poisson's ratio; γ, engineering material constant

References

1. Roy, S., Dey, S., Khutia, N., Chowdhury, A. R., & Datta, S. (2018). Design of patient specific dental implant using FE analysis and computational intelligence techniques. *Applied Soft Computing, 65*, 272–279.

2. Macedo, J. P., Pereira, J., Faria, J., Pereira, C. A., Alves, J. L., Henriques, B., Souza, J. C. M., & Lopez-Lopez, J. (2017). Finite element analysis of stress extent at peri-implant bone surrounding external hexagon or Morse taper implants. *Journal of the Mechanical Behavior of Biomedical Materials, 71*, 441–447.

3. Hasan, I., Röger, B., Heinemann, F., Keilig, L., & Bourauel, C. (2012). Influence of abutment design on the success of immediately loaded dental implants: experimental and numerical studies. *Medical Engineering & Physics, 34*, 817–825.

4. Cavallaro, J., & Greenstein, G. (2011). Angled implant abutments: a practical application of available knowledge. *Journal of the American Dental Association (1939), 142*, 150–158.

5. Okumura, N., Stegaroiu, R., Nishiyama, H., Kurokawa, K., Kitamura, E., Hayashi, T., et al. (2011). Finite element analysis of I plant-embedded maxilla model from CT data: comparison with the conventional model. *Journal of Prosthodontic Research, 55*, 24–31.

6. Tian, K., Chen, J., Han, L., Yang, J., Huang, W., & Wu, D. (2012). Angled abutments result in increased or decreased stress on surrounding bone of single-unit dental I plants: a finite element analysis. *Medical Engineering & Physics, 34*, 1526–1531.

7. Adell, R., Lekholm, U., Rockler, B., & Branemark, P. I. (1981). 15-Year.Study of osseointegrated implants in the treatment of the edentulous jaw. *Journal of Oral Surgery, 10*, 387–416.

8. Branemark, R., Branemark, P. I., Rydevik, B., & Myers, R. (2001). Osseointegration in skeletal reconstruction and rehabilitation. A review. *Journal of Rehabilitation Research and Development, 38*(2), 175–181.

9. Branemark, P. I., Breine, U., Adell, R., Hansson, O., Lindstom, J., & Ohlsson. (1969). Intra-osseous anchorage of dental prostheses. I. Experimental studies. *Scandinavian Journal of Plastic and Reconstructive Surgery, 3*, 81–100.

10. Branemark, P. I. (1983). Osseointegration and its experimental background. *The Journal of Prosthetic Dentistry, 50*(3), 399–410.

11. Schenk, R. K., & Buser, D. (1998). Osseointegration: a reality. *Periodontology, 2000, 17*, 22–35.

12. Vanegas-Acosta, J. C., Landinez P, N. S., Garzón-Alvarado, D. A., & Casale R, M. C. (2011). A finite element method approach for the mechanobiological modeling of the osseoinegration of a dental implant. *Computer Methods and Programs in Biomedicine, 101*, 297–314.

13. Taylor, D., Hazenberg, J. G., & Lee, T. C. (2007). Living with cracks: damage and repair in human bone. *Nature Materials, 6*(4), 263–268.

14. Gao, J., Xu, W., & Ding, Z. (2006). 3D finite element mesh generation of complicated tooth model based on CT slices. *Computer Methods and Programs in Biomedicine, 82*(2), 97–105.

15. Van Eijden, T. M. (2000). Biomechanics of the mandible. *Critical Reviews in Oral Biology and Medicine, 11*(1), 123–136.

16. Gačnik, F., Ren, Z., & Hren, N. I. (2014). Modified bone density-dependent orthotropic material model of human mandibular bone. *Medical Engineering & Physics, 361*, 684–1692.

17. Ding, X., Liao, S.-h., Zhu, X.-h., Wang, H.-m., & Zou, B.-j. (2015). Effect of orthotropic material on finite element modeling of completely dentate mandible. *Materials and Design, 84*, 144–153.

18. Wirtz, D. C., Pandorf, T., Portheine, F., Radermacher, K., Schiffers, N., Prescher, A., et al. (2003). Concept and development of an orthotropic FE model of the proximal femur. *Journal of Biomechanics, 36*(2), 289–293.

19. Peng, L., Bai, J., Zeng, X., & Zhou, Y. (2006). Comparison of isotropic and orthotropic material property assignments on femoral finite element models under two loading conditions. *Medical Engineering & Physics, 28*, 227–233.

20. Lengsfeld, M., Schmitt, J., Alter, P., Kaminsky, J., & Leppek, R. (1998). Comparison of geometry-based and CT voxel-based finite element modeling and experimental validation. *Medical Engineering & Physics, 20*(7), 515–522.

21. Kluess, D., Souffrant, R., Mittelmeier, W., Wree, A., Schmitz, K.-P., & Bader, R. (2009). A convenient approach for finite-element-analyses of orthopedic implants in bone contact: modeling and experimental validation. *Computer Methods and Programs in Biomedicine, 95*, 23–30.

22. Wirtz, D. C., Schiffers, N., Pandorf, T., Radermacher, K., Weichert, D., & Forst, R. (2000). Critical evaluation of known bone material properties to realize anisotropic FE-simulation of the proximal femur. *Journal of Biomechanics, 33*(10), 1325–1330.

23. Rho, J. Y., Hobatho, M. C., & Ashman, R. B. (1995). Relations of mechanical properties to density and CT numbers in human bone. *Medical Engineering & Physics, 17*(5), 347–355.

24. Taddei, F., Pancanti, A., & Viceconti, M. (2004). An improved method for the automatic mapping of computed tomography numbers onto finite element models. *Medical Engineering & Physics, 26*(1), 61–69.

25. Keyak, J. H., & Falkinstein, Y. (2003). Comparison of in situ and in vitro CT scan based finite element model predictions of proximal femoral fracture load. *Medical Engineering & Physics, 25*(9), 781–787.

26. Taylor, W. R., Roland, E., Ploeg, H., Hertig, D., Klabunde, R., Warner, M. D., et al. (2002). Determination of orthotropic bone elastic constants using FEA and modal analysis. *Journal of Biomechanics, 35*(6), 767–773.

27. Dhatrak, P., Shirsat, U., Sumanth, S., & Deshmukh, V. (2018). Finite element analysis and experimental investigations on stress distribution of dental implants around implant-bone interface. *Materials Today: Proceedings, 55*, 641–5648.

28. Dhatrak, P., Shirsat, U., Deshmukh, V., Sumanth, S. (2018) Fatigue life prediction of commercial dental implant using analytical approach and verification by FEA, Proceedings of Fatigue, Durability and Fracture Mechanics, Lecture Notes in Mechanical Engineering 203–212.

29. ABAQUS, Version 6.7 Documentation, ABAQUS Analysis Manual, Simulia, Dassault Systems, RI, USA 2007.

30. San Antonio, T., Ciaccia, M., Muller-karger, C., & Casanova, E. (2012). Orientation of Orthotropic material properties in a femur FE model: a method based on the principal stresses directions. *Medical Engineering & Physis, 34*, 914–919.

31. Jalali, S. K., Yarmohammadi, R., & Maghsoudi, F. (2016). Finite element stress analysis of functionally graded dental implant of a premolar tooth. *Journal of Mechanical Science and Technology, 30*(11), 4919–4923.

32. Zykova, Y., Kudryavtseva, V., Gai, M., Kozelskaya, A., Frueh, J., Sukhorukov, G., & Tverdohlebov, S. (2019). Free-standing microchamber arrays as a biodegradable drug depot system for implant coatings. *European Polymer Journal, 114*, 72–80. https://doi.org/10.1016/j.eurpolymj.2019.02.029.

33. Gai, M., Kurochkin, M. A., Li, D., Khlebtsov, B. N., Dong, L., Tarakina, N., Poston, R., Gould, D. J., Frueh, J., & Sukhorukov, G. B. (2018). In-situ NIR-laser mediated bioactive substance delivery to single cell for EGFP expression based on biocompatible microchamber-arrays. *Journal of Controlled Release, 276*, 84–92. https://doi.org/10.1016/j.jconrel.2018.02.044.

34. Gai, M., Frueh, J., Kudryavtseva, V. L., Yashchenok, A. M., & Sukhorukov, G. B. (2017). Polylactic acid sealed polyelectrolyte multilayer microchambers for entrapment of salts and small hydrophilic molecules precipitates. *ACS Applied Materials & Interfaces, 9*, 16536–16,545. https://doi.org/10.1021/acsami.7b03451.

35. Gai, M., Li, W., Frueh, J., & Sukhorukov, G. B. (2019). Polylactic acid sealed polyelectrolyte complex microcontainers for controlled encapsulation and NIR-laser based release of cargo. *Colloids and Surfaces. B, Biointerfaces, 173*, 521–528. https://doi.org/10.1016/j.colsurfb.2018.10.026.

36. Ipek Karacan, I., Macha, G., Choi, S., & Cazalbou, B. (2017). Ben-Nissan, antibiotic containing poly lactic acid/hydroxyapatite biocomposite coatings for dental implant applications. *Key Engineering Materials, 758*, 120–125. https://doi.org/10.4028//www.scientific.net//KEM.758.120.

37. Kim, S., Myung, W.-C., Lee, J.-S., Chai, J.-K., Jung, U.-W., Yang, H.-C., Lee, I.-S., & Choi, S.-H. (2011). The effect of fibronectin-coated implant on canine osseointegration. *Journal of Periodontal Implant Science, 41*, 242–247. https://doi.org/10.5051/jpis.2011.41.5.242.